Article

Using Modified Remote Sensing Imagery to Interpret Changes in Cultivated Land under Saline-Alkali Conditions

Hui Gao [1,2], Jintong Liu [1,*], A. Egrinya Eneji [3], Lipu Han [1] and Limei Tan [1]

[1] Key Laboratory of Agricultural Water Resources, Center for Agricultural Resources Research,
Institute of Genetics and Developmental Biology, Chinese Academy of Sciences, Shijiazhuang 050022, China;
gaohui0110@163.com (H.G.); lpuhan@ sjziam.ac.cn (L.H.); tanlimei@sjziam.ac.cn (L.T.)

[2] University of Chinese Academy of Sciences, Beijing 100049, China

[3] Department of Soil Science, Faculty of Agriculture, University of Calabar, Calabar PMB 1115, Nigeria;
aeeneji@yahoo.co.uk

[*] Correspondence: jtliu@sjziam.ac.cn; Tel./Fax: +86-311-8587-1749

Abstract: Managing the rapidly changing saline-alkali land under cultivation in the coastal areas of China is important not only for mitigating the negative impacts of such land on the environment, but also for ensuring long-term sustainability of agriculture. In this light, setting up rapid monitoring systems to assist decision-making in developing sustainable management plans is therefore an absolute necessity. In this study, we developed a new interpretation system where symbols are used to grade and classify saline-alkali lands in space and time, based on the characteristics of plant cover and features of remote sensing images. The system was used in combination with the maximum likelihood supervised classification to analyze the changes in cultivated lands under saline-alkali conditions in Huanghua City. The analysis revealed changes in the area and spatial distribution of cultivated under saline-alkali conditions in the region. The total area of saline-alkali land was 139,588.8 ha in 1992 and 134,477.5 ha in 2011. Compared with 1992, severely and moderately saline-alkali land areas decreased in 2011. However, non/slightly saline land areas increased over that in 1992. The results showed that the salinization rate of arable lands in Huanghua City decreased from 1992 to 2011. The moderately saline-alkali land southeast of the city transformed into non/slightly saline-alkaline. Then, severely saline-alkali land far from the coastal zone west of the city became moderately saline-alkaline. Spatial changes in cultivated saline-alkali lands in Huanghua City were such that the centers of gravity (CG) of severely and non/slightly saline-alkali land moved closer the coastline, while that of the moderately saline-alkali land moved from southwest coastal line to northwest. Factors influencing changes in cultivated lands in the saline-alkali ecosystem included climate, hydrology and human activity. Thus, studies are required to further explore these factors in order to build a better understanding into the relative contributions of the changes saline-alkali state on the functions of coastline ecosystems.

Keywords: saline-alkali ecosystem; cultivated land; remote sensing image interpretation; modified method

1. Introduction

Globally, some 83 million hectares of land is affected by salt, with a wide range of distribution in five continents and over 100 countries [1]. Soil salinization is so much so extensive that it now spreads at the rate of two million hectares per year [2,3]. This requires the development of effective preventive

and management measures, including rapid reliable means of getting information on spatial and temporal distributions of saline-alkali lands across the globe.

Remote sensing techniques and data are widely used to detect and map salt-affected areas [4–6]. Dwivedi and Rao [7] noted that the combination of Landsat TM bands 1, 3 and 5 was most suitable for the interpretation of salt-affected soils. Dwivedi and Sreenivas [8] believed that a substantial understanding of saline-alkali lands could be developed through principal component analysis, image differencing and band rationing. Metternichet and Zinck [9] used remote sensing images in combination with field survey and laboratory data to analyze the distribution of soil salinization. The choice of the time of remote sensing image is critical for the extraction of reliable soil salinization data. The spatial and temporal distributions of soil salinization in Jiefangzha Irrigation Sub-district were determined by analyzing remote sensing images acquired at the end of March. The irrigation sub-district is in the western part of Hetao Irrigation District in Inner Mongolia, China [10]. Then, Wang [11] used remote sensing images for August and September to extract data on the salinization of the delta oasis of Weigan and Kuqa rivers.

In this study, we used remote sensing images acquired at the end of May or the beginning of June to determine the spatial and temporal variability of soil salinity in a coastal area in Huanghua City. At the time, soils with different levels of salts were under different vegetation covers of different reflectivity. As the features of each land use class in the composite TM images was clearly delineated in the standard false color, the images did not require complex transformation and index calculations in order to interpret the features. We developed an interpretation symbol system to grade and classify saline-alkali soils based on vegetation characteristics. The system was developed using data from site investigation, plant cover characteristics and remote sensing features. We used TM remote sensing image of standard false color composite (band 4, 3 and 2) without any complex image transformation and index calculation. Finally, the interpretation system was integrated with the maximum likelihood supervised classification method to derive relevant on saline-alkali soils.

2. Materials and Methods

2.1. Study Site

The west Bohai Sea in Huanghua City is part of a coastal alluvial plain in Hebei Province, China (Figure 1), covering a vast area of saline-alkali land in the region. The total area of the city is 220,000 ha, a large proportion (129,462.3 ha) of which is cultivated. The main land cover includes water, marshland and residential land, with respective areas of 34,675.3 ha, 25,752.2 ha and 18,103.8 ha. The other forms of land cover account for a very small fraction of the study area [12]. The climate in the study area is warm temperate, semi-humid monsoon, with a mean annual precipitation of about 627 mm, occurring mainly between July and September. The mean annual potential evaporation is 1980 mm. The area, which is prone to summer drought and spring waterlogging, has shallow groundwater salinity of above 3 g/L. As there is lack of freshwater in the study area, it is mainly covered by salt-resistant vegetation.

2.2. Data Source

The remote sensing data, including two sets of Landsat (Row123/Path 32 of the WRS-2) and Thematic Mapper (TM) images (dated 27 May 1992 and 1 June 2011), were downloaded from the public domain [13]. The Landsat scenes were acquired under clear sky conditions at the end of May or beginning of June. To eliminate bias in the comparison of the multi-temporal datasets, the data were referenced to a common coordinate grid. Image-to-image calibration was adopted and TM image with accurate geometric correction taken as reference image. In addition, data for 1992 and 2011 were geo-referenced to UTM coordinate system and the accuracy controlled within 0.5 grid (with 1 grid = 30 m × 30 m). The geographic referenced data were then clipped to the study area in ARCGIS.
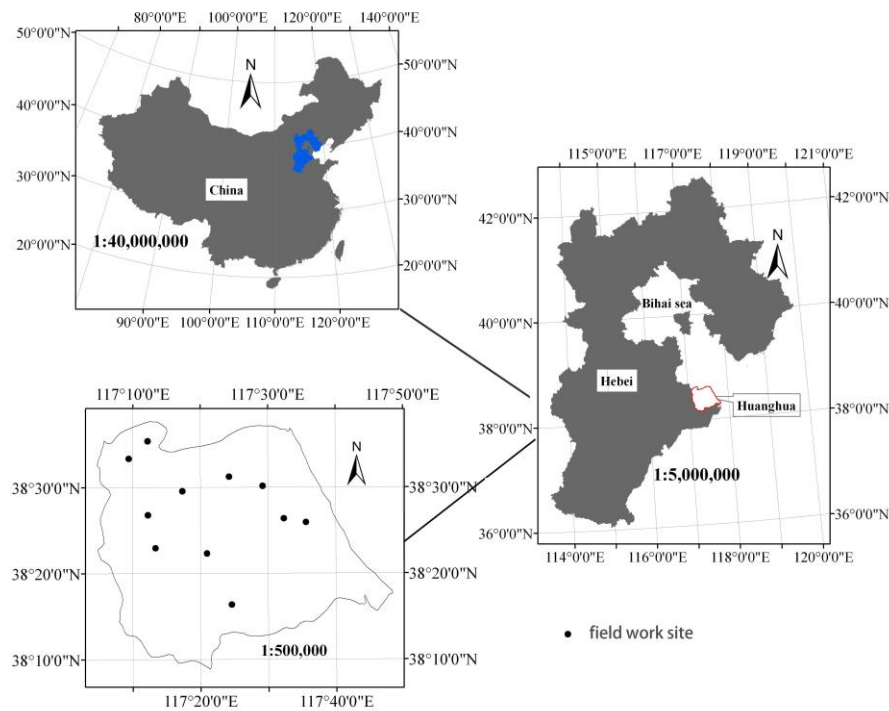
Figure 1. Map of China depicting the location depicting Hebei Province (**top left**), that of the province depicting the study area (**right**) and an expanded map of the study area (**bottom left**).

2.3. Methods

A modified remote sensing imagery was used to interpret changes in cultivated lands under saline-alkali conditions in Huanghua City. The schematic representation of the modified method used to process the remote sensing images is depicted in Figure 2.
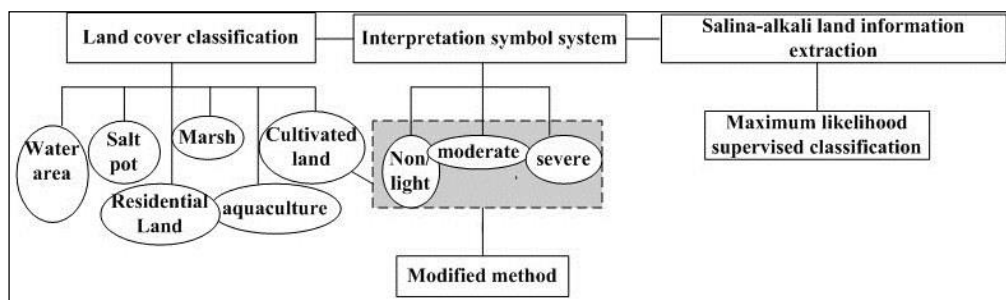

Figure 2. A schematic representation of the method of modification of the remote sensing imagery used in the study.

Maximum likelihood Supervised classification was used to analyze land classification. Maximum likelihood classification (MLC) [14] is a method for determining a known class of distributions as the maximum for a given statistic. An assumption of normality is made for the training samples. The algorithm builds the probability density functions for each category. During classification, all unclassified pixels are assigned membership based on the relative likelihood (probability) of that pixel occurring within each category's probability density function [15].

Suppose there are *G* predefined categories, the unclassified image possesses m bands. According to Bayesian formula, the posterior probability of category *k*, *P(Gk/x)* is defined as:

$$P\left(G_k/x\right) = \frac{P\left(x/G_k\right)P\left(G_K\right)}{P\left(x\right)} \tag{1}$$

where *P(Gₖ)* is the prior probability of category *k*; *P(x/Gk)* is conditional probability of observing *x* from G_k (probability density function); and *P(x)* is the same for each category. If we have no knowledge about the prior distributions *P(Gₖ)*, then we can assume that all categories are probable. Therefore, the likelihood function is determined by *P(x/Gₖ)*, which is also called the likelihood of G_k with respect to x. Given the logarithm, the discriminant function can be expressed as:

$$M_k\left(x\right) = LnP\left(G_k\right) + Ln\frac{/S_k^{-1}/^{1/2}}{\left(2\pi\right)^{\mathbf{m}/2}} - 1/2\left(x - u_k\right)^T S_k^{-1}\left(x - u_k\right) \tag{2}$$

where $x = [x_1, x_2, \ldots, x_m]^T$ is the vector of a pixel; $M_k(x)$ is the likelihood function of *x* belonging to category *k*; and μ_k and S_k are the mean vector and covariance matrix of the *K*th category.

A post-classification comparison was used to analyze land use changes. Here, the matrix tool in the image interpreter module of ERDAS IMAGINE software was used to get the map of spatial changes in a land use and transition matrix of different land use classes land for 1992–2011.

Then the center of gravity migration model was used to describe the overall intensity of change as well as the spatial variation characteristics of different degrees of the saline-alkali land. The spatial migration of the gravity center was demonstrated by the change in gravity center coordinate [16–18]. The gravity center coordinate was calculated as:

$$X = \frac{\sum_{j=1}^{n} P_j X_j}{P_j} \tag{3}$$

$$Y = \frac{\sum_{j=1}^{n} P_j Y_j}{P_j} \tag{4}$$

where *X* and *Y* are the gravity center coordinate for cultivated land under saline-alkali conditions in the Huanghua City (°), P_j is the area of the *j*th patch (ha), X_j and Y_j are gravity center coordinate of the *j*th patch (°), and *n* is the number of patches in the cultivated lands under saline-alkali conditions.

3. Modified Remote Sensing Imagery

3.1. Saline-Alkali Land Classification

The land use in Huanghua City was divided into the following six classes based on the state land use classification standard [19]. The classes included water body, salt pot, residential land, aquaculture and cultivated land. Cultivated land was further divided into three classes based on spectral signatures of land covers—severely saline-alkali land, moderately saline-alkali land and non/lightly saline-alkali land (Figure 3).
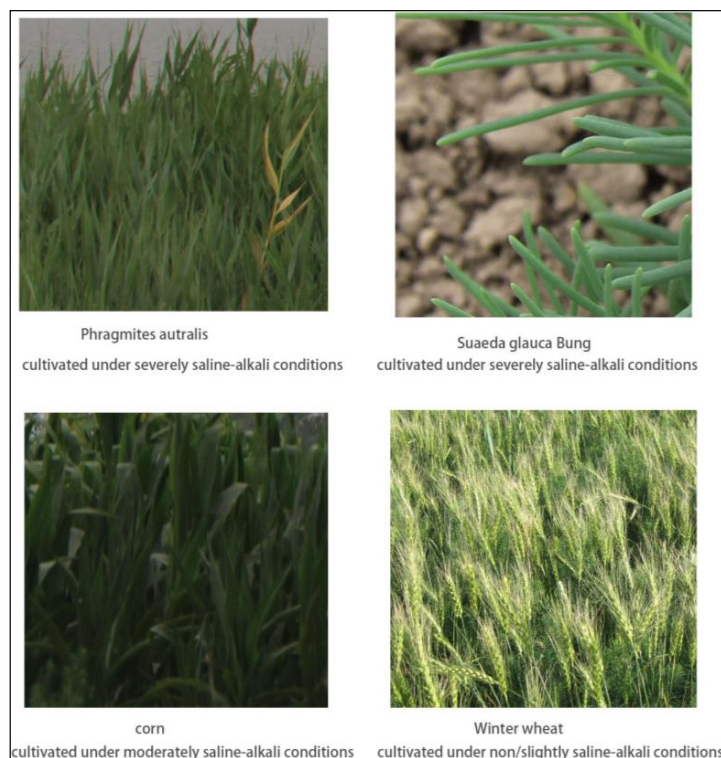
Figure 3. Photos of different classes of saline-alkali lands taken in the field in 2011.

3.2. New Interpretation Symbol System

To determine the spatial and temporal changes in cultivated lands under saline-alkali conditions in the coastal region, a new interpretation symbol system consistent with the saline-alkali land classification was set up. Zhang [20] defined the classes of saline-alkali soils for Northeast China and developed an interpretation symbol system that combined image element (color) with spatial location. Dwivedi [21] set up an interpretation symbol system that combined image elements (color, texture, pattern, shape, size, association, etc.) and laboratory analysis of field soil samples data. The interpretation symbol system used in this study is based on site investigation, plant cover characteristics and remote sensing images features (Table 1). We used the spectral signature of characteristic plants in coastal cultivated land for the end of May or early June. It was driven by the vegetation characteristics at the site during the time of study. Severely saline-alkali lands were covered by salt-resistant vegetation such as *Suaeda glauca Bunge* and *Phragmites autralis* (Figure 3), which was almost brown but had sporadic red. Moderately saline-alkali lands were covered by spring corn or cotton (Figure 3), with apparent gray and red image features in the ratio of about 50%. The image feature of winter wheat planted in non/slightly saline-alkali lands (Figure 3) was apparently red.

Table 1. Classes of saline-alkali lands in Huanghua City and the interpretation symbols of TM (standard false color composite).

Classes of Saline-Alkali Land	Vegetation Feature	Image Feature
Severely saline-alkali land	Salt-resistant vegetation	
Moderately saline-alkali land	Spring corn, cotton	
Non/slightly saline-alkali land	Winter wheat	

3.3. Classification Templates

The training sets about water body, salt pot, residential land and aquaculture were selected based on the national land survey. The training sets in 1992 and 2011 were obtained based on the first and second national land survey, respectively. The training sets about cultivated land under saline-alkali condition using visual interpretation were selected using based on the new interpretation symbol system in 1992 and 2011. Training samples were selected for each class in order to establish the classification templates. Over ten training samples were merged for each final class. The contingency matrix tool was used to evaluate the classification templates, and the related error matrix given as Tables 2 and 3. In 1992, Classification accuracy of other classes is over 90%, except for marsh and aquaculture. In 2011, Classification accuracy of other classes is over 90%, except for marsh only. Classification accuracy of each class in templates was less than 15% in 1992 and 2011, so the classification templates were considered to be successful.

3.4. Saline-Alkali Land Information Extraction

Based on the classification templates, the land use classification maps were established using maximum likelihood supervised method in the ERDAS IMAGINE software (Intergraph Corporation, Huntsville, AL, USA) (Figure 4). The maps of spatial and temporal variations in the saline-alkali lands were obtained through post-classification comparison in ARCGIS environment (Figure 8).
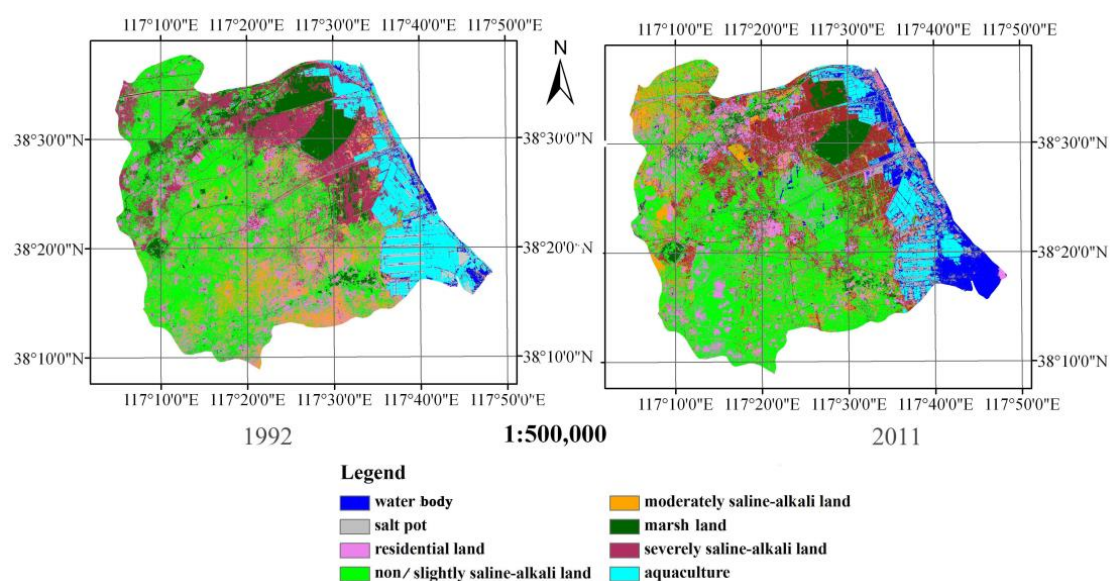

Figure 4. Land use maps for the period 1992 and 2011 in Huanghua City, Hebei Province.

3.5. Validation of Remote Sensing Interpretation

We use statistical yearbook and previous research to verify accuracy of the land use classification maps of 1992 and field survey to verify accuracy of the land use classification maps of 2011. According to statistical yearbook and previous research [22], the area of cultivated land was about 130,000 ha. The area of cultivated land is 139,588.8 ha by analyzing the land use classification map of 1992. They are about consistent. We choose 11 sites in the land use classification map of 2011 and did field investigation through Global Position System (GPS) in 2011. The land use classes of the 11 field sites matched well with interpretation results.

Table 2. Error matrix for the classifications of land use in 1992 in Huanghu City, China (unit: pixel).

Classification	Severely	Moderately	Non/Slightly	Residential Land	Marsh Land	Aquaculture	Salt Pot	Water
Severely	1509	0	19	26	28	1	0	0
Moderately	8	1562	67	70	6	0	0	0
Non/slightly	25	0	1126	4	94	0	0	0
Residential land	3	15	6	1141	24	1	3	0
Marsh land	3	0	2	0	1091	0	0	0
Aquaculture	0	0	0	0	0	657	3	38
Salt pot	0	0	0	0	1	3	370	1
Water	0	0	0	0	0	14	38	552
Total	1548	1577	1220	1241	1244	676	414	591
Classifications accuracy	97.48	99.05	92.30	91.94	87.70	97.19	89.37	93.40

Table 3. Error matrix for the classifications of land use in 2011 in Huanghu City, China (unit: pixel).

Classification	Severely	Moderately	Non/Lightly	Residential Land	Marsh Land	Aquaculture	Salt Pot	Water
Severely	355	49	37	23	9	0	2	0
Moderately	7	1362	81	89	6	0	0	0
Non/slightly	1	25	1500	22	51	0	0	0
Residential land	6	53	21	1691	99	1	3	0
Marsh land	1	0	7	4	1300	0	0	0
Aquaculture	0	0	0	4	3	1808	0	0
Salt pot	0	0	0	0	0	3	449	39
Water	0	0	0	10	0	71	16	605
Total	370	1489	1646	1843	1468	1883	470	644
Classifications accuracy	95.95	91.47	91.13	91.75	88.56	96.02	95.53	93.94

4. Results

4.1. Temporal Changes in Arable Saline-Alkali Land

The dynamics of soil salinization in the severely, moderately and non/slightly saline-alkali lands for the period from 1992 to 2011 are plotted in Figure 4. From the satellite images for 1992 and 2011, we the different classes of cultivated land areas and the related ratios (%) to the total area were statistically demarcated in ARCGIS environment. Figure 5 shows the different classes of cultivated areas as percentages of total cultivated area and Figure 6 shows the changes in area in the different classes for 1992–2011. As in Figure 2, there were changes in the other classes of land use in 1992–2011 in the study area. Residential land area was increased by 27.86% from 25,521.6 ha to 32,631.7 ha during 1992–2011. Aquaculture area shrunk, decreasing from 23,065.5 ha in 1992 to 13,468.5 ha in 2011. The area of salt spot increased from 6512.8 ha to 7684.4 ha. Area under water bodies significantly increased from 4362.8 ha to 17,070.8 ha over the 20-years period. Marshland area also decreased from 18,998.2 ha in 1992 to 11,716.6 ha in 2011 in Huanghua City in Hebei Province, China.
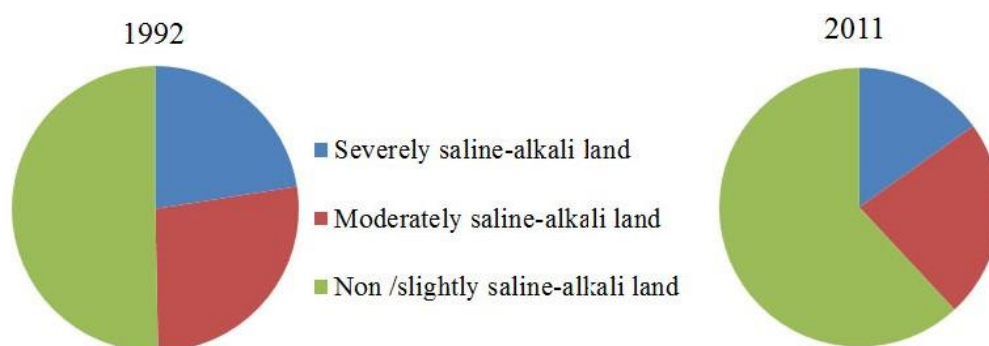

Figure 5. Ratio of the areas of land under different saline-alkali land classes as percentages of total cultivated areas in 1992 and 2011 in Huanghua City in Hebei Province, China.
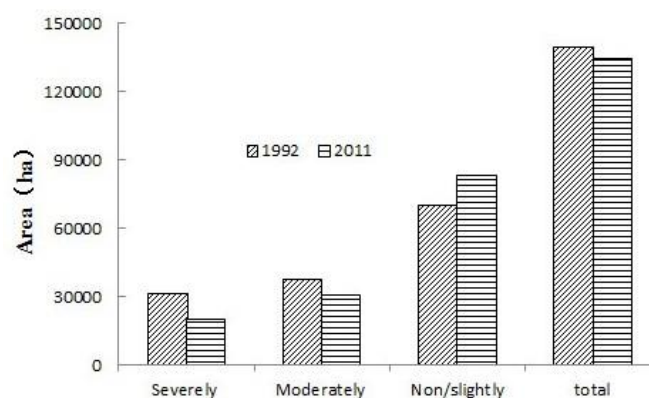

Figure 6. Temporal changes in the areas of land under different saline-alkali land classes from the period from 1992 to 2011 in Huanghua City in Hebei Province, China.

For the period from 1992 to 2011, the total area of saline-alkali lands decreased by 3.66% from 139,588.8 ha to 134,477.5 ha, respectively. The area under severely saline-alkali lands changed the most (35.2%), decreasing from 31,425.8 ha in 1992 to 20,373.2 ha in 2011. The area under moderately saline-alkali lands had a similar trend as that under severely saline-alkali lands, decreasing by 18.7% from 37,984.8 ha in 1992 to 30,888.2 ha in 2011. However, non/lightly saline-alkali lands had the reverse trend, increasing by 18.6% from 70,178.1 ha to 83,216.1 ha.

The changes in ratios of the areas of land under different saline-alkali land classes as percentages of total cultivated areas in 1992 and 2011 were also analyzed. The areas under severely and moderately

saline-alkali lands as percentage of the total cultivated land area decreased from 22.5 to 15.1% and from 27.2% to 23.0%, respectively. The area under non/slightly saline-alkali lands increased by 11.6% for the period from 1992 to 2011 (Figure 5). It suggested that there was a drop in the degree of salinization of arable lands in Huanghua City, China.

As in Tables 2 and 3, the error in each class of the classification templates was less than 15%, which influenced the classification results. For example, the classifications accuracies of marshland were 87.7% and 88.56% for 1992 and 2011, respectively, so the area of marsh is less than the actual area. Although, other land use classes also had similar issues. However, this form of error did not compromise the overall trend of changes in land use the study area.

4.2. Spatial Changes in Saline-Alkali Arable

Figure 4 shows the spatial distribution of saline-alkali land in the study area in 1992 and 2011. It is clear that the severely saline-alkali lands were concentrated in the east of Huanghua City, near the coast. Most of the moderately saline-alkali lands were in the south of the city in 1992, largely shifting to the north of the city in 2011. The non/slightly saline-alkali lands occurred far from the coast.

The characteristics of the spatial changes in saline lands can be explained not only qualitatively (using land use maps), but also statistically (using the changes in different land use classes). The detected characteristics in land salinization in 1992–2011 are depicted in Figure 7 and the change matrix detailed in Table 4. From the change matrix (Table 4), it was clear that 24,770.6 ha of moderately saline-alkali lands and 7470.18 ha of severely saline-alkali lands were converted into non/slightly saline-alkali lands in the study area. In addition, 3575.16 ha of severely saline-alkali lands were converted into moderately saline-alkali lands in the region over the same period. Furthermore, 12,125.1 ha and 6540.3 ha of non/slightly saline lands were converted into moderately and heavily saline-alkali lands, respectively. Similarly, 2234.9 ha of moderately saline-alkali lands were converted into severely saline-alkali lands.
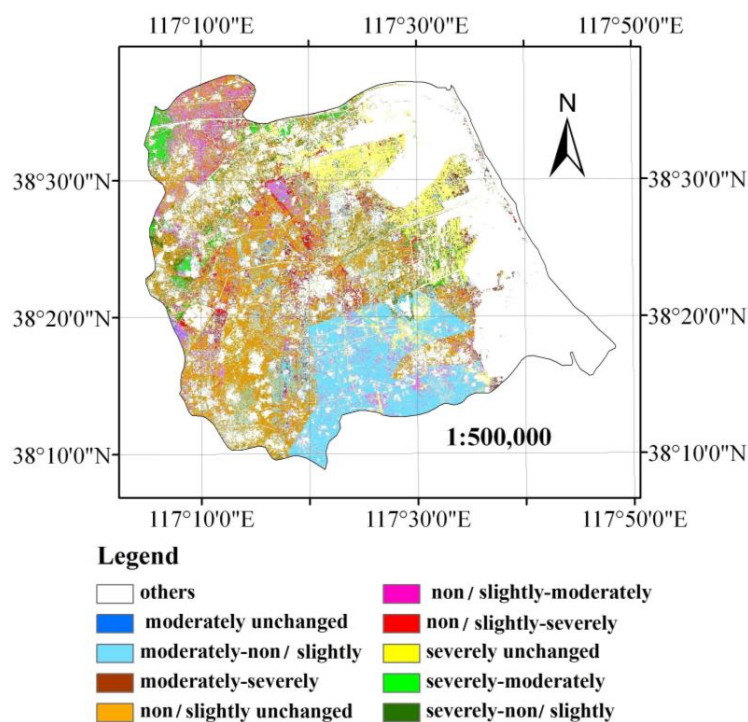

Figure 7. Spatial changes in land use for the period 1992–2011 in Huanghua City, China.

Generally, land conversion was mainly between moderately and non/slightly saline-alkali lands. Moreover, land conversion among the different classes of saline-alkali lands resulted in an overall

decline in the area of land under moderately and severely saline-alkali conduction. In other words, land salinization in Huanghua City decreased from 1992 to 2011. As seen in Table 4, 3704.22, 562.87 and 3645.99 ha of marshland was converted into non/slightly, moderately and heavily saline-alkali lands, respectively. Meanwhile, some cultivated land under non/lightly, moderately and severely saline-alkali conditions were converted into marshland. Some cultivated lands were also converted into residential lands. Although errors exist in the values reported above, such errors are not large enough to affect the overall dynamics of land use change in the study area.

The changes in the different land use classes were also analyzed using centroid shift for the period from 1992 to 2011. The moderately saline-alkali lands in southeast Huanghua City were converted into non/slightly saline-alkaline lands, and severely saline-alkali lands far from the coast (west of the city) converted into moderately saline-alkaline lands (Figure 7). The changes in the center of gravity for the different classes cultivated lands under saline-alkali condition (Figure 8). For 1992–2011, the gravity center of cultivated land under severely and non/slightly saline-alkali conditions shifted 3.47 km and 9.55 km towards the southeast, respectively. Cultivated lands under moderately saline-alkali conditions shifted 31.89 km towards the northwest. The center of gravity of severely and non/slightly saline-alkali land shifted closer towards the coastline, while that of moderately saline-alkali lands shifted from the southwest coastline towards the northwest.
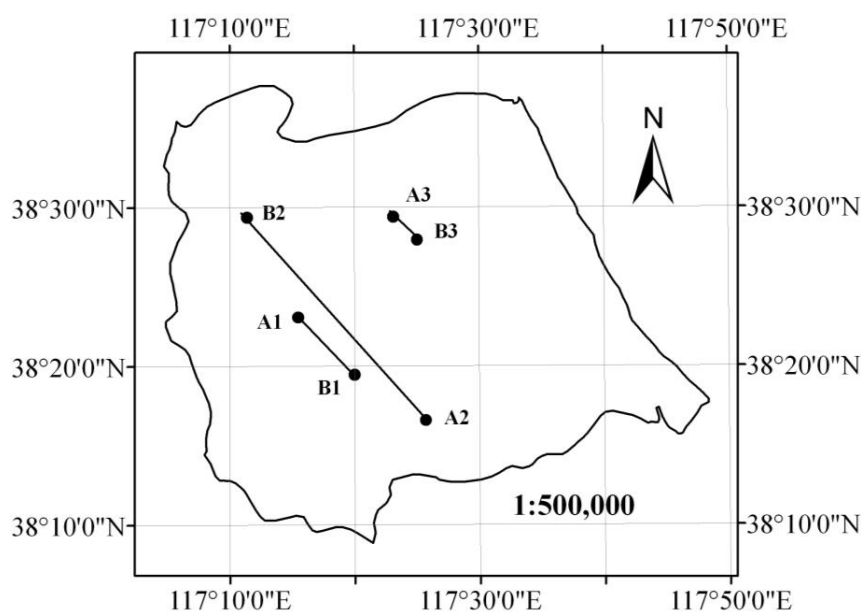

Figure 8. Centers of gravity of cultivated lands under saline-alkali conditions in Huanghua City of Hebei Province, China. Note that: A1 is center of gravity of cultivated lands under non or light saline-alkali conditions in 1992; A2 is centers of gravity of cultivated lands under moderately saline-alkali conditions in 1992; A3 is centers of gravity of cultivated lands under severely saline-alkali conditions in 1992; B1 is centers of gravity of cultivated lands under non or lightly saline-alkali conditions in 2011; B2 is centers of cultivated lands under gravity of moderately saline-alkali conditions in 2011; and B3 is centers of gravity of cultivated lands under severely saline-alkali conditions in 2011.

Table 4. Change matrix of the conversion of one land use class into another (ha) during the period from 1992 to 2011 in Huanghua City of Hebei Province, China (ha).

Classes	Non/Lightly	Moderately	Severely	Residential Land	Marsh Land	Salt Pot	Water Body	Aquaculture
Non/lightly	38746.9	12125.1	6540.3	10139.2	1756.26	253.53	486.9	129.96
Moderately	24770.6	1187.55	2243.88	2408.4	135.45	236.16	316.62	127.08
Severely	7470.18	3575.16	14930.5	6701.85	874.61	746.01	362.24	1324.17
Residential land	8204.76	2805.03	2838.78	10419.7	227.88	436.59	425.07	163.8
Marsh land	3704.22	561.87	3645.99	1669.77	8685.63	61.29	268.65	400.77
Salt pot	291.78	68.76	255.24	573.84	12.42	2280.06	2558.25	472.41
Water body	18.99	21.24	272.88	346.32	20.52	2538.27	9342.63	10504.6
Aquaculture	8.64	28.53	160.56	372.6	3.78	1132.47	2310.48	345.69

5. Discussions

5.1. Method Feasibility

Largely, image acquisition period decides image features. The specific seasons of image acquisition highlight research objectives and procedures. Guan and Liu [23] noted that images acquired in May were critical for distinguishing different classes of land use in the Yellow River Delta. In the Huanghua City study area, the specific season of images acquisition is end of May or early June. During this time, different classes of cultivated land have distinct vegetation characteristic. The high contrast in image features during this time makes the classification process very successful.

In this study, the classification accuracy of the templates exceeded 90%. The exceptions only were marsh and salt pot, which were developed based on the national land survey and the new interpretation symbol system (Tables 3 and 4). By combining the classification templates with the maximum likelihood supervised classification method, information was derived on cultivated lands under saline-alkali conditions in the coastal ecosystem of Huanghua City. This information was used to analyze the area and spatial distribution of cultivated land under saline-alkali conditions in 1992–2011. A total of 11 field sites were identified in the land use map for Huanghua City in 2011. The land use classes of the 11 field sites matched well with interpretation results.

The total area of cultivated land under saline-alkali conditions was 91,100 ha. The proportions of non/slightly (salinity < 0.3%), moderately (0.3% < salinity < 0.5%) and severely (salinity > 0.5%) saline-alkali lands in 2006 were 81.67%, 12.55% and 5.77%, respectively [22]. The total area of cultivated land under saline-alkali lands land were 70,987 ha, with proportions of non/slightly, moderately and severely saline-alkali lands in 2011 of 61.9%, 23% and 15.1%, respectively. The order of the proportion of each class of land use was non/slightly > moderately > severely. The accuracy of all the classes was high and therefore reasonable. The results showed that salinization of cultivated lands in the Huanghua city study area dropped during the period from 1992 to 2011 [24]. Thus, the new interpretation symbol system and its classification system were suitable for analysis of spatial and temporal variations in saline-alkali lands in coastal regions. The modified remote sensing imagery characteristics were dynamic in real-time and suitable for an accurate monitoring of large areas. The method was also labor, time and cost efficient compared with conventional field measurements [3,25,26].

Vegetation classes as indicators for salinity had strong correlation with electrical conductivity. In this study, climate was not significant factor driving vegetation growth and distribution in the study area. Because this was surprising, it requires further research to more accurately determine the role of climate in the growth and distribution of vegetation in cultivated lands under saline-alkali conditions.

5.2. Changes in Cultivated Lands

Soil texture and irrigation water quality influence the soil salinity. Climate, terrain features and groundwater table also cause soil salinization. Then, human activity aggravates soil salinization to different levels [27–29]. Soil salinization has obvious seasonal characteristics, as dramatic increase in evaporation (due to high spring temperatures) results in salt deposition. Soil desalination occurs in summer due to soil eluviation driven by summer rains. The low rainfall in autumn coupled with low temperatures results in low vaporization and salt deposition. When soils become frozen in wheat fields and groundwater depth steadily drops, the result is low salt accumulation.

Groundwater depth sits at about 0.5–4 m below the land surface, with salinity above 5 g/L in most regions. In the study area, groundwater supplements soil water and soil salt because of its shallow depth and high salinity. Since the 1960s, authorities in Huanghua City have embarked on the construction of drainage systems in cultivated lands to improve saline-alkali condition. The drainage systems consist of networks of ditches, which convey water to and from the field. There is 8 m width ditch in every 50 m wide field. However, the drainage system northwest of Huanghua City has a series of problems including deposition, blocking, falling depth, reduced flow, etc. Most frustrating among the problems is the rapid rate at which the drains have been filled by sedimentation. Drainage

and its related problems have favored increase in groundwater level. Decreasing groundwater depth enhances soil salinization. However, the drainage system southeast of Huanghua City has remained intact since 1992. This has meant a decreasing groundwater level and low soil salinization.

6. Conclusions

In this paper, a modified method was developed for application in interpreting changes in remote sensing images for cultivated land under saline-alkali conditions in coastal regions. The modified method was a new interpretation symbol system for grading and classifying cultivated land under saline-alkali conditions. The system was developed based on site investigation, plant cover characteristics and remote sensing images features. Then, classification templates were established based on the interpretation symbol system and the maximum likelihood supervised classification used to generate land use maps for Huanghua City in Hebei Province China.

The total area of saline-alkali land decreased during the period from 1992 to 2011 in Huanghua City, hence a drop in the degree of salinization of arable land in the city. The spatial distribution of saline-alkali land changed with time and the center of gravity of severely, moderately and non/slightly saline lands changed as well. The center of gravity of severely and non/slightly saline-alkali lands shifted closer towards the coastline, whereas that of moderately saline-alkali lands shifted from the southwest coastline towards the northwest.

Author Contributions: Hui Gao and Jintong Liu conceived the concept of the paper; Hui Gao analyzed the data; Lipu Han and Limei Tan contributed the analysis tools used; and Hui Gao and A. Egrinya Eneji wrote the paper.

Conflicts of Interest: The authors declare no conflict of interest.

References

1. Martinez-Beltran, J.; Manzur, C.L. Overview of salinity problems in the world and FAO strategies to address the problem. In Proceedings of the International Salinity Forum, Riverside, CA, USA, 25–27 April 2005; pp. 311–313.
2. Rengasamy, P. World salinization with emphasis on Australia. *J. Exp. Bot.* **2006**, *57*, 1017–1023. [CrossRef] [PubMed]
3. Abbas, A.; Khan, S.; Hussain, N.; Hanjra, M.A.; Akbar, S. Characterizing soil salinity in irrigated agriculture using a remote sensing approach. *Phys. Chem. Earth* **2013**, *55–57*, 43–52. [CrossRef]
4. Metternicht, G.I. Catwgeorical fuzziness: A comparison between crisp and fuzzy class boundary modeling for mapping salt-affected soils using Landsat TM data and a classification based on anion ratios. *Ecol. Model.* **2003**, *168*, 371–389. [CrossRef]
5. Farifteh, J.; Farshad, A.; George, R.J. Assessing salt-affected soil using remote sensing solute modeling, and geophysics. *Geoderma* **2006**, *130*, 191–206. [CrossRef]
6. Masoud, A.A.; Koike, K. Arid land salinization detected by remotely-sensed landcover changes: A case study in the Siwa region, NW Egypt. *J. Arid. Environ.* **2006**, *66*, 151–167. [CrossRef]
7. Dwivedi, R.S.; Rao, B.R.M. The selection of the best possible Landsat TM band combination for delineating salt-affected soils. *Int. J. Remote Sens.* **1992**, *13*, 2051–2058. [CrossRef]
8. Dwivedi, R.S.; Sreenivas, K. Delineation of salt-affected soils and waterlogged areas in the Indo-Gangetic plains using IRS-1C LISS-III data. *Int. J. Remote Sens.* **1998**, *19*, 2739–2751. [CrossRef]
9. Metternichet, G.I.; Zinck, J.A. Spatial discrimination of salt- and sodium-affected soils surfaces. *Int. J. Remote Sens.* **1997**, *18*, 2571–2586. [CrossRef]
10. Yu, R.; Liu, T.; Xu, Y.; Zhu, C.; Zhang, Q.; Qu, Z.; Liu, X.; Li, C. Analysis of salinization dynamics by remote sensing in Hetao Irrigation District of North China. *Agric. Water Manag.* **2010**, *97*, 1952–1960. [CrossRef]
11. Wang, H.; Fan, Y.; Tashpolat, T. The research of soil salinization human impact based on remote sensing classification in oasis irrigation area. *Procedia Environ. Sci.* **2011**, *10*, 2399–2405.

12. Yuan, Y. A study on ecosystem services value for 38° N ecological transect of Hebei Province. Ph.D. Thesis, University of Chinese Academy of Sciences, China, June 2012. (In Chinese)

13. Geospatial Date Cloud. Available online: http://www.gscloud.cn/sources/?cdataid=263&pdataid=10 (accessed on 10 December 2013).

14. Sun, J.; Yang, J.; Zhang, C.; Yun, W.; Qu, J. Automatic remotely sensed image classification in a grid environment based on the maximum likelihood method. *Math. Comp. Model.* **2013**, *58*, 573–581. [CrossRef]

15. Hagner, O.; Reese, H. A method for calibrated maximum likelihood classification of forest types. *Remote Sens. Environ.* **2007**, *110*, 438–444. [CrossRef]

16. Bao, Y.; Wulantuya, H.; Xiang, B.; Zhao, X.L. Studies on the movement of farmland gravity and analyses of its driving factors in Inner Mongolia. *China Prog. Geogr.* **1998**, *17*, 47–54.

17. Duan, H.; Tao, W.; Xue, X.; Liu, S.; Guo, J. Dynamics of aeolian desertification and its driving forces in the Horqin Sandy Land, Northern China. *Environ. Monit. Assess.* **2014**, *186*, 6083–6096. [CrossRef] [PubMed]

18. Liu, X.; Dong, G.; Xigang, W.; Xue, Z.; Jiang, M.; Lu, X.; Zhang, Y. Characterizing the spatial pattern of marshlands in the Sanjiang Plain, Northeast China. *Ecol. Eng.* **2013**, *53*, 335–342. [CrossRef]

19. GB/T 21010-2007. Available online: http://www.biaozhun8.cn/so.asp?k=GT%2FB21010-2007 (accessed on 29 June 2016). (In Chinese)

20. Zhang, S.-W.; Yang, J.-C.; Li, Y.; Zhang, Y.-Z.; Chang, L.-P. Change of saline-alkali land in northeast China and its causes since the mid-1950s. *J. Nat. Res.* **2010**, *25*, 435–442. (In Chinese)

21. Dwivedi, R.S.; Sreeniv, K.; Ramana, K.V. Inventory of salt-affected soils and water logged areas: A remote sensing approach. *Int. J. Remote Sens.* **1999**, *20*, 1589–1599. [CrossRef]

22. Yue, Y.-J.; Zhang, F.; Zhang, G.-M.; Zhang, H.; Xu, P.-H.; Wang, J.-A. Coastal saline-alkali land use change and its optimization. *Res. Sci.* **2010**, *32*, 423–430. (In Chinese)

23. Guan, Y.X.; Liu, G.H. Remote sensing detection of dynamic variation of the saline land in the yellow river delta. *Remote Sens. Land Resour.* **2003**, *2*, 19–22. (In Chinese)

24. Ma, T.J.; Zhao, M.R.; Matsumoto, S.; Yamazaki, J. Evolution of saline-alkali soils in Heilong-gang region. *Acta Pedologica Sinica* **1995**, *32*, 228–234. (In Chinese)

25. Ibrahimi, M.K.; Miyazaki, T.; Nishimura, T.; Imoto, H. Contribution of shallow groundwater rapid fluctuation to soil salinization under arid and semiarid climate. *Arab. J. Geosci.* **2014**, *7*, 3901–3911. [CrossRef]

26. Jin, X.M.; Vekerdy, Z.; Zhang, Y.-K.; Liu, J.T. Soil Salt content and its relationship with crops and groundwater depth in the Yinchuan Plain (China) using remote sensing. *Arid. Land Res. Manag.* **2010**, *26*, 227–235. [CrossRef]

27. Kairis, C.; Kosmas, C.; Karavitis, C.; Ritsema, L.; Salvati, S.; Acikalin, M.; Alcala, P.; Atlhopheng, J.; Barrera, J.; Belgacem, A.; et al. Evaluation and selection of indicators for land degradation and desertification monitoring: Types of degradation, causes, and implications for management. *Environ. Manag.* **2014**, *54*, 971–982. [CrossRef] [PubMed]

28. Konukcu, F.; Gowing, J.W.; Rose, D.A. Dry drainage: A sustainable solution to waterlogging and salinity problems in irrigation areas? *Agric. Water Manag.* **2006**, *83*, 1–12. [CrossRef]

29. Zhang, Z.; Abuduwaili, J.; Yimit, H. The occurrence, sources and spatial characteristics of soil salt and assessment of soil salinization risk in Yanqi Basin, Northwest China. *PLoS ONE* **2014**, *9*, 1–12. [CrossRef] [PubMed]